Safe Sequential Trajectory Planning of Multi-Vehicle Systems via Hamilton-Jacobi-Isaacs Variational Inequality

Mo Chen, Jaime F. Fisac, Shankar Sastry, Claire J. Tomlin

Abstract— We consider the problem of planning trajectories for a group of N vehicles, each aiming to reach its target set while avoiding danger zones of other vehicles. The analysis of problems like this is extremely important practically, especially given the growing interest in utilizing unmanned aircraft systems for civil purposes. The direct solution of this problem by solving a single-obstacle Hamilton-Jacobi-Isaacs (HJI) variational inequality (VI) is numerically intractable due to the exponential scaling of computation complexity with problem dimensionality. Furthermore, the single-obstacle HJI VI cannot directly handle situations in which vehicles do not have a common scheduled arrival time. Instead, we perform sequential trajectory planning by considering vehicles in order of priority, modeling higher-priority vehicles as time-varying obstacles for lower-priority vehicles. To do this, we solve a double-obstacle HJI VI which allows us to obtain the reach-avoid set, defined as the set of states from which a vehicle can reach its target while staying within a time-varying state constraint set. From the solution of the HJI VI, we can also extract the latest start time and the optimal control for each vehicle. This is a first application of the double-obstacle HJI VI which can handle systems with time-varying dynamics, target sets, and state constraint sets, and results in computation complexity that scales linearly, as opposed to exponentially, with the number of vehicles in consideration.

I. INTRODUCTION

Consider a group of autonomous vehicles trying to perform a task or reach a goal which may be time-varying in the joint state space of the vehicles. In addition, the vehicles must avoid obstacles, and other vehicles. Providing safety and performance guarantees for such a multi-agent autonomous system is very relevant practically. Unmanned aerial vehicles (UAVs), for example, have in the past been used mainly for military operations [1]. However, recently, there has been a growing interest in using UAVs for civil applications, as companies like Amazon and Google are looking in the near future to send unmanned aerial vehicles into the airspace to deliver packages [2], [3]. Because of this, government agencies such as the FAA are also expressing growing interest in analyzing these problems in order to prevent airspace conflicts that could arise with the introduction of potentially many UAVs in an urban environment [4]. In addition, UAVs can be used not only to deliver packages quickly, but in any situation where fast response is desired. For example, UAVs

All authors are with the Department of Electrical Engineering and Computer Sciences, University of California, Berkeley. {mochen72, jfisac, sastry, tomlin}@eecs.berkeley.edu

can provide emergency supplies to disaster-struck areas that are otherwise difficult to reach [5].

In general, multi-agent systems are difficult to analyze due to their inherent high dimensionality. For example, the joint state space of 10 vehicles would have 30 dimensions even if each vehicle is described by a simple model with three states. Multi-vehicle systems also often involve aspects of cooperation and asymmetric goals among the vehicles or teams of vehicles, making their analysis particularly interesting. Despite these difficulties, it is still important to analyze multi-agent autonomous systems because of their applications in robotics and aircraft safety.

Multi-agent autonomous systems have been explored extensively in the literature. Some researchers have done work on multi-vehicle path planning in the presence of other unknown vehicles or moving entities with assumptions on their specific control strategies [6]. In a number of formulations for safe multi-vehicle navigation, these assumed strategies induce velocity obstacles that vehicles must avoid to maintain safety [7], [8]. Researchers have also used potential functions to perform collision avoidance while maintaining formation given a predefined trajectory [9], [10]. However, these bodies of work have not considered trajectory planning and collision avoidance simultaneously.

One well-known technique for optimal trajectory planning under disturbances or adversaries is reachability analysis, in which one computes the reach-avoid set, defined as the set of states from which the system can reach a target set while remaining within a state constraint set for all time. For reachability of systems of up to five dimensions, single-obstacle Hamilton-Jacobi-Isaacs (HJI) variational inequalities (VI) [11], [12] have been used in situations where obstacles and target sets are static. Another HJI VI formulation [13] is able to handle moving target sets with no obstacles.

A major practical appeal of the above approaches stems from the availability of modern numerical tools such as [11], [14], [15], [16], which can efficiently solve HJI equations when the problem dimension is low. These numerical tools have been successfully used to solve a variety of differential games, path planning problems, and optimal control problems, including aircraft collision avoidance [11], automated in-flight refueling [17], and two-player reach-avoid games [18]. The advantage of the HJI approaches is that they can be applied to a large variety of system dynamics, and provide guarantees on the system's safety and performance.

Despite the power of the previous HJI formulations, the approaches become numerically intractable very quickly as the number of vehicles in the system is increased. This is

because the numerical computations are done on a grid in the joint state space of the system, resulting in an exponential scaling of computation complexity with respect to the dimensionality of the problem. Furthermore, state constraint sets, while useful for modeling unsafe vehicle configurations, are required to be time-invariant in [11], [19], [12]. To solve problems involving time-varying state constraints, [20] proposed to augment state space with time; however, this introduces an extra state space dimension without addressing the added computation complexity.

Recently, [21] presented a double-obstacle HJI VI which handles problems in which the dynamics, target sets, and state constraint sets are all time-varying, and provided a numerical implementation based on well-known schemes. The formulation does not introduce any additional computation overhead compared to the above-mentioned techniques, while maintaining the same guarantees on the system's safety and performance. In this paper, we provide a first application of the theory presented in [21].

Our contributions in this paper are as follows. First, we formulate a multi-vehicle collision avoidance problem involving N autonomous vehicles. Each vehicle seeks to get to its own target sets while avoiding collision with all other vehicles. To reduce the problem complexity to make the problem tractable, we assign a priority to each vehicle, and model higher-priority vehicles as time-varying obstacles that need to be avoided. We then utilize the double-obstacle HJI VI proposed in [21] to compute reach-avoid sets to plan trajectories for vehicles in order of priority. This way, we are able to offer a tractable solution that scales linearly, as opposed to exponentially, with the number of vehicles. We compare our approach to the traditional HJI approach involving static obstacles in a simple two-vehicle system, and demonstrate the scalability of our approach in a more complex four-vehicle system.

II. PROBLEM FORMULATION

Consider N vehicles $P_i, i = 1 \ldots, N$, each trying to each one of N target sets $\mathcal{T}_i, i = 1 \ldots, N$, while avoiding collision with each other. Each vehicle i has states $\mathbf{x}_i \in \mathbb{R}^{n_i}$ and travels on a domain $\Omega = \Omega_{obs} \cup \Omega_{free}$, where Ω_{obs} represents the obstacles that each vehicle must avoid, and Ω_{free} represents all other states in the domain at which vehicles can move. Each vehicle $i = 1, 2, \ldots, N$ moves with the following dynamics for $t \in [t_i^{\text{EST}}, t_i^{\text{STA}}]$:

$$\dot{\mathbf{x}}_i = f_i(t, \mathbf{x}_i, \mathbf{u}_i), \quad \mathbf{x}_i(t_i^{\text{LST}}) = \mathbf{x}_i^0 \qquad (1)$$

where $\mathbf{x}_i^0$ represents the initial condition of vehicle i, $\mathbf{u}_i(\cdot)$ represents the control functions of vehicle i. In general, $f_i(\cdot, \cdot, \cdot)$ depends on the specific dynamic model of vehicle i, and need not be of the same form across different vehicles. Denote $\mathbf{p}_i$ the subset of the states $\mathbf{x}_i$ that represent the position of the vehicle. Given $\mathbf{p}_i^0 \in \Omega_{free}$, we define the admissible control function set for P_i to be the set of all control functions such that $\mathbf{p}_i(t) \in \Omega_{free} \forall t \geq 0$. Denote the joint state space of all vehicles $\mathbf{x} \in \mathbb{R}^n$ where $n = \sum_i n_i$, and their joint control $\mathbf{u}$.
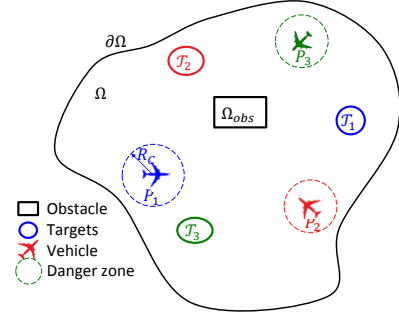

Fig. 1: An illustration of the problem formulation with 3 vehicles. Each vehicle P_i seeks to reach its target set $\mathcal{T}_i$ by time $t = t_i^{\text{STA}}$, while avoiding physical obstacles Ω_{obs} and the danger zones of other vehicles.

We assume that the control functions $\mathbf{u}_i(\cdot)$ are drawn from the set $\mathbb{U}_i := \{\mathbf{u}_i : [t_i^{\text{LST}}, t_i^{\text{STA}}] \to \mathcal{U}_i, \text{measurable}^1\}$ where $\mathcal{U}_i \in \mathbb{R}^{n_i^{\mathbf{u}}}$ is the set of allowed control inputs. Furthermore, we assume $f_i(t, \mathbf{x}_i, \mathbf{u}_i)$ is bounded, Lipschitz continuous in $\mathbf{x}_i$ for any fixed $t, \mathbf{u}_i$, and measurable in $t, \mathbf{u}_i$ for each $\mathbf{x}_i$. Therefore given any initial state $\mathbf{x}_i^0$ and any control function $\mathbf{u}_i(\cdot)$, there exists a unique, continuous trajectory $\mathbf{x}_i(\cdot)$ solving (1) [22].

The goal of each vehicle i is to arrive at $\mathcal{T}_i \subset \mathbb{R}^{n_i}$ at some scheduled time of arrival (STA) t_i^{STA} in minimum time, while avoiding danger with all other vehicles. Vehicle i must arrive at $\mathcal{T}_i$ at or before t_i^{STA}. The target sets $\mathcal{T}_i$ can be used to represent desired kinematic quantities such as position and velocity and, in the case of non-holonomic systems, quantities such as heading angle. t_i^{EST} can be interpreted as the earliest start time (EST) of vehicle i, which may only depart from its initial state at or after t_i^{EST}. Further, we define t_i^{LST}, the latest (acceptable) start time (LST) for vehicle i. Our problem can now be thought of as determining the LST t_i^{LST} for each vehicle such that each vehicle can get to $\mathcal{T}_i$ at or before the STA t_i^{STA}, and finding a control to do this safely. If the EST is before the LST $t_i^{\text{LST}} < t_i^{\text{EST}}$, then it is infeasible for vehicle i to arrive at $\mathcal{T}_i$ at or before the STA t_i^{STA}. In general, comparing t_i^{LST} and t_i^{EST} is feasibility problem that may arise in practice; however, for simplicity of presentation, we will assume that $t_i^{\text{EST}} \leq t i_i$.

Danger is described by sets $\mathcal{D}_{ij}(\mathbf{x}_j) \subset \Omega$. In general, the definition of $\mathcal{D}_{ij}$ depends on the conditions under which vehicles i and j are considered to be in a unsafe configuration, given the state of vehicle j. In this paper, we define danger to be the situation in which the two vehicles come within a certain radius R_C of each other: $\mathcal{D}_{ij}(\mathbf{x}_j) = \{\mathbf{x}_i : \|\mathbf{p}_i - \mathbf{p}_j\|_2 \leq R_C\}$. Such a danger zone is also used in [23].

An illustration of the problem setup is shown in Figure 1.

In general, the analysis of the above problem in general must be done in the joint state space of all vehicles, making

---

the analysis computationally intractable. In this paper, we will instead consider the problem of performing path planning of the vehicles in a sequential manner. Without loss of generality, we consider the problem of first fixing $i = 1$ and determining the optimal control for vehicle 1, the vehicle with the highest priority. The resulting optimal control $\mathbf{u}_1$ sends vehicle 1 to $\mathcal{T}_1$ in minimum time.

Then, we plan the minimum time trajectory for each vehicle $2, \ldots, N$, in decreasing order of priority, given the previously-determined trajectories for higher-priority vehicles $1, \ldots, i - 1$. We assume that all vehicles have complete information about the states and trajectories of all other vehicles, and that all vehicles adhere to their planned trajectories. Thus, in planning its trajectory, vehicle i treats higher-priority vehicles $1, \ldots, i - 1$ as time-varying obstacles.

With the above sequential path planning (SPP) protocol and assumptions, our problem now reduces to the following for vehicle i. Given $\mathbf{x}_j(\cdot), j = 1, \ldots, i - 1$, determine $\mathbf{u}_i(\cdot)$ that maximizes t_i^{LST} and such that $x_i(t_i^{\text{STA}}) \in \mathcal{T}_i$.

III. SOLUTION VIA DOUBLE-OBSTACLE HJI VI AND SPP

One direct way of solving the problem formulated in Section II is by solving a corresponding single-obstacle HJI VI [11], [12]. In this approach, one considers the joint time-invariant dynamics of the entire system, $f(\mathbf{x}, \mathbf{u})$, and defines the static goal set and the static avoid set in the joint state space of all vehicles. The goal set encodes the joint states representing all vehicles being at their target sets, and the avoid set encodes the joint states representing all unsafe configurations. These sets are defined as sub-zero level sets of appropriate implicit surface functions $s(\mathbf{x})$ where $\mathbf{x} \in \mathcal{S} \Leftrightarrow s(\mathbf{x}) \leq 0$. Having defined the implicit surface functions, the HJI VI (2) is then solved backwards in time with the implicit surface function representing the terminal set $l(\mathbf{x})$ as the initial condition and the implicit surface function representing the avoid set $a(\mathbf{x})$ as a constraint to obtain the reach-avoid set $\mathcal{RA}$, which defines the set of states from which the system has a control to drive the state to the goal set $\mathcal{L}$ while staying out of the avoid set $\mathcal{A}$ all times. Note that the joint dynamics, goal set, and avoid set must be time-invariant. Time-varying dynamics and sets can be treated by augmenting the state space with time as an auxiliary state [20]; however, this state augmentation comes at a large computational expense.

$$\max \left\{ \frac{\partial V}{\partial t} + \min \left[0, H \left(\mathbf{x}, \frac{\partial V}{\partial \mathbf{x}} \right) \right], -a(\mathbf{x}) \right\} = 0,$$
$$V(\mathbf{x}, 0) = l(\mathbf{x}) \tag{2}$$

where the optimal Hamiltonian is given by

$$H(\mathbf{x}, p) = \min_{\mathbf{u} \in \mathcal{U}} p \cdot f(\mathbf{x}, \mathbf{u}).$$

The direct solution described above has been successfully used to solve a number of problems involving up to a pair of vehicles [11], [17], [18], [24]. However, since the numerical methods for solving a PDE or a VI involve gridding up the state space, the computation complexity scales

exponentially with the number of dimensions in the joint state. This makes the single-obstacle HJI VI inapplicable for problems involving three or more vehicles. Therefore, instead of solving a single-obstacle HJI VI in the joint state space in $\mathbb{R}^n = \mathbb{R}^{\sum_i n_i}$, we will consider the problem in in $\mathbb{R}^{n_i}$ and solve a sequence of *double-obstacle* HJI VIs introduced in [21]. By doing so, we take advantage of the fact that time-varying targets, obstacles, and dynamics can be handled by the double-obstacle HJI VIs (but not by the single-obstacle HJI VI without incurring significant computational expense), making the analysis of the problem tractable. Furthermore, even if the dimensionality of the problem is sufficiently low for computing a numerical solution to the single-obstacle HJI VI, its inability to handle time-varying systems would still limit us to only consider problems in which the required time of arrival is common to all vehicles: $t_i^{\text{STA}} = t^{\text{STA}} \ \forall i$.

We first describe the framework for computing reach-avoid sets with arbitrary terrain, domain, moving obstacles, and moving target sets based on [21]. As with the single-obstacle HJI VI, sets are defined as sub-zero level sets of implicit surface functions; however, crucially, these implicit surface functions can be time-varying in the HJI VI without increasing computational complexity. Being able to compute reach-avoid sets with moving obstacles allows us to overcome the computational intractability described above by sequentially performing path planning for one vehicle at a time in order of priority, while treating higher-priority vehicles as moving obstacles. The target set is defined in the same way as in the single-obstacle HJI VI; the avoid set is by convention defined as the complement of the state constraint set in the double-obstacle HJI VI.

A. Reachability via HJI VI

We first state the result given in [21], and then specialize the result to the problem formulation given in Section II. Consider a general nonlinear system describing the state evolution of two players in a differential game for $t \in [0, T]$.

$$\dot{x}(t) = f(t, x, u, d), \quad x(0) = x \tag{3}$$

where x is the joint state, u is the control input for player 1, and d is the control input for player 2. Their joint dynamics f is assumed to be Lipschitz continuous in x for any fixed u, d and t. Given control functions $u(\cdot), d(\cdot)$, there exists a unique trajectory $\phi_x^{u,d}((\tau), \tau)$ [25]. Player 1 wishes to minimize, and player 2 to maximize the following cost functional:

$$\mathcal{V}(t, x, u(\cdot), d(\cdot))$$
$$= \min_{\tau \in [t,T]} \max \left\{ l(\phi_{x(0)}^{u,d}(\tau), \tau), \max_{s \in [t, \tau]} g(\phi_{x(0)}^{u,d}(s), s) \right\} \tag{4}$$

The value of the game is given by

$$V(x, t) := \sup_{u(\cdot)} \inf_{\delta[u](\cdot)} \mathcal{V}(x, t, u(\cdot), \delta[u](\cdot)) \tag{5}$$

where player 2 chooses a nonanticipative strategy $d(\cdot) = \delta[u](\cdot)$, under which player 2 chooses a control signal $d(t)$ in

response to player 1's control function up to time t, $u(\tau), \tau \leq t$ [19]. The value of the game characterizes reach-avoid set, or all the states from which player 1 can reach the target $\mathcal{L}$ encoded by the implicit surface function $l(x,t)$, while staying within some state constraint set $\mathcal{G}$ encoded by the implicit surface function $g(x,t)$, despite the adversarial actions of player 2. The value function is the unique viscosity solution [26] to the following HJI VI [21]:

$$
\begin{aligned}
\max \Big\{ \min \big\{ & \partial_t V + H^\pm\left(x, D_x V, t\right), l(x,t) - V(x,t) \big\} \\
& g(x,t) - V(x,t) \Big\} = 0, \quad t \in [0,T], \quad x \in \mathbb{R}^n \\
& V(x,T) = \max\left\{ l(x,T), g(x,T) \right\}, \quad x \in \mathbb{R}^n
\end{aligned}
\tag{6}
$$

The proof is given in [21] and is based on viscosity solution theory [27], [28].

Now consider the system with dynamics given by (1). Given a time-varying target set $\mathcal{T}_i(t)$, we define an implicit surface function $l(\mathbf{x}_i, t)$ such that $\mathbf{x}_i \in \mathcal{T}_i(t) \Leftrightarrow l_i(\mathbf{x}_i, t) \leq 0$. Given a time-varying obstacle $\mathcal{A}_i(t)$ that vehicle i must avoid, we define the implicit surface function $g_i(\mathbf{x}_i, t)$ such that $\mathbf{x} \notin \mathcal{A}_i(t) \Leftrightarrow g_i(x,t) \leq 0$. With the above definitions, the problem formulated in Section II is equivalent to the optimal control problem in which vehicle i chooses a control function $\mathbf{u}_i(\cdot)$ to minimize the following cost functional:

$$
\begin{aligned}
& \mathcal{V}_i\big(t, \mathbf{x}_i, \mathbf{u}_i(\cdot)\big) \\
& = \min_{\tau \in [t,T]} \max \left\{ l_i(\mathbf{x}_i(\tau), \tau), \max_{s \in [t,\tau]} g_i(\mathbf{x}_i(s), s) \right\}
\end{aligned}
\tag{7}
$$

Note here, we have an optimal control problem involving only one vehicle and no adversary, unlike in the case of the HJI VI (6). Now, specializing (6) to our optimal control problem, the value function that characterizes the reach-avoid set $\mathcal{RA}_i(t)$ is $V_i(\mathbf{x}_i, t)$, where $\mathbf{x}_i \in \mathcal{RA}_i(t) \Leftrightarrow V_i(\mathbf{x}_i, t) \leq 0$. $V_i(\mathbf{x}_i, t)$ is the viscosity solution [26] of the HJI VI

$$
\begin{aligned}
\max \Big\{ \min \big\{ & \partial_t V_i + H_i\left(\mathbf{x}_i, D_{\mathbf{x}_i} V_i, t\right), l_i(\mathbf{x}_i, t) - V_i(\mathbf{x}_i, t) \big\} \\
& g_i(\mathbf{x}_i, t) - V_i(\mathbf{x}_i, t) \Big\} = 0, t \in [t_i^{\text{EST}}, t_i^{\text{STA}}], \mathbf{x}_i \in \mathbb{R}^{n_i} \\
& V_i(\mathbf{x}_i, t_i^{\text{STA}}) = \max\left\{ l_i(\mathbf{x}_i, t_i^{\text{STA}}), g_i(\mathbf{x}_i, t_i^{\text{STA}}) \right\}, \quad \mathbf{x}_i \in \mathbb{R}^{n_i}
\end{aligned}
\tag{8}
$$

where the Hamiltonian $H_i(t, \mathbf{x}_i, p)$ is given by

$$
H_i(t, \mathbf{x}_i, p) = \min_{\mathbf{u}_i \in \mathcal{U}_i} p \cdot f_i(t, \mathbf{x}_i, \mathbf{u}_i)
\tag{9}
$$

From the Hamiltonian, we can obtain the optimal control:

$$
\mathbf{u}_i^* = \arg\min_{\mathbf{u}_i} H_i(t, \mathbf{x}_i, p)
\tag{10}
$$

B. Sequential Path Planning

In order to use (8) to perform SPP, we first define the moving obstacles induced by higher-priority vehicles. Specifically, for vehicle i, we define the moving obstacles $\mathcal{O}_j^i(t)$ induced by vehicles $j = 1, \ldots, i-1$, given their known trajectories $\mathbf{x}_j(\cdot)$, to be

$$
\mathcal{O}_j^i(t) := \{\mathbf{x}_i : \mathbf{p}_i \in \mathcal{D}_{ij}(\mathbf{x}_j(t))\}
\tag{11}
$$

Each vehicle i must avoid being in $\mathcal{O}_j^i(t)$ for each $j = 1, \ldots, i-1$ and for all time t, as well as avoid being in static obstacles Ω_{obs} in the domain. Therefore, for the ith vehicle, we compute the reach-avoid set with the following time-varying avoid set $\mathcal{A}_i(t)$ and goal set $\mathcal{L}_i(t)$:

$$
\begin{aligned}
& \mathcal{A}_i(t) := \{\mathbf{x}_i : \mathbf{p}_i \in \Omega_{obs}\} \cup \left(\bigcup_{j=1,\ldots,i-1} \mathcal{O}_j^i(t) \right) \\
& \mathcal{L}_i(t) := \mathcal{T}_i, t \leq t_i^{\text{STA}}
\end{aligned}
\tag{12}
$$

The goal set is represented by the implicit surface function $l_i(\mathbf{x}, t)$, where $l_i(\mathbf{x}_i, t) \leq 0 \Leftrightarrow \mathbf{x}_i(t) \in \mathcal{L}_i(t)$. The state constraint set in the HJI VI is defined as the complement of the avoid set, $\mathcal{A}_i^c(t)$, and is represented by the implicit surface function $g(\mathbf{x}_i, t)$, where $g(\mathbf{x}_i, t) \leq 0 \Leftrightarrow \mathbf{x}_i \notin \mathcal{A}_i(t)$. For both $l_i(\mathbf{x}_i, t)$ and $g(\mathbf{x}_i, t)$, we use the signed distance function (in $\mathbf{x}_i$) to the sets $\mathcal{L}_i(t)$ and $\mathcal{A}_i^c(t)$, respectively.

Now, we can solve the HJI VI (8). The solution $V(\mathbf{x}_i, t)$ represents the reach-avoid set $\mathcal{RA}(t)$: $V(\mathbf{x}_i, t) \leq 0 \Leftrightarrow \mathbf{x}_i(t) \in \mathcal{RA}(t)$. $\mathcal{RA}(t)$ is the set of states at starting time t from which vehicle i can arrive at $\mathcal{T}_i$ at time t_i^{STA} while avoiding obstacles and danger zones of all higher-priority vehicles $j = 1, \ldots, i-1$.

Alternatively, given an initial state $\mathbf{x}_i^0$, we can solve (8) to some $t_i^{\text{LST}} = \inf\{t : \mathbf{x}_i^0 \in \mathcal{RA}(t)\}$. This represents the latest time that vehicle i must depart from its initial position in order to reach $\mathcal{T}_i$ while avoiding all danger zones of higher-priority vehicles $j = 1, \ldots, i-1$.

The optimal control is given by

$$
\mathbf{u}_i(t) = \arg\min H_i\left(t, \nabla_{\mathbf{x}_i} V(\mathbf{x}_i, t), V(\mathbf{x}_i, t)\right)
\tag{13}
$$

Observe that since each vehicle i is guaranteed to be safe with respect to higher priority vehicles $j = 1, \ldots, i-1$, the safety of all vehicles, including lower-priority vehicles, can also be guaranteed.

IV. NUMERICAL IMPLEMENTATION

For the numerical examples in this paper, we use a numerical method provided in [21] which is based on methods in [11], [14]. The numerical algorithm is shown in Algorithm 1. Here, $\mathbf{i}$ represents the index for a particular grid cell, I represents the set of grid indices, and k represents the time step. $\hat{V}$ represents the numerical approximation to V. $D_x^+ \hat{V}, D_x^- \hat{V}$ represent the "right" and "left" approximations of spatial derivatives. For the numerical Hamiltonian $\hat{H}$, we used the well-known Lax-Friedrich approximation [19], [29].

For the spatial derivatives $D_x^\pm \hat{V}$, we used a fifth-order accurate weighted essentially nonoscillatory scheme [29], [30]. For the time derivative $D_t \hat{V}$, we used a third-order total variation diminishing Runge-Kutta scheme [30], [31]. For these derivative approximations, the implementation in [16] is used. For two-, three-, and four-dimensional (2D, 3D, 4D) computations, we used a $200^2, 71^3, 45^4$ grid, respectively.

Algorithm 1: Numerical Double-Obstacle HJI Solution

> **Data**: $\hat{l}(x_\mathbf{i}, t_\mathbf{k}), \hat{g}(x_\mathbf{i}, t_\mathbf{k})$
> **Result**: $\hat{V}(x_\mathbf{i}, t_\mathbf{k})$
>
> Initialization
> **for** $\mathbf{i} \in I$ **do**
> **Init** $\quad\Big\lfloor \; \hat{V}(x_\mathbf{i}, t_0) \leftarrow \max\{\hat{l}(x_\mathbf{i}, t_0), \hat{g}(x_\mathbf{i}, t_0)\};$
> Value propagation
> **for** $k \leftarrow 1$ **to** n **do**
> $\quad$ **for** $\mathbf{i} \in I$ **do**
> $\qquad \hat{V}(x_\mathbf{i}, t_k) \leftarrow \hat{V}(x_\mathbf{i}, t_{k-1})$
> $\qquad\quad + \displaystyle\int_{t_k}^{t_{k-1}} \hat{H}\big(x_\mathbf{i}, D_x^+\hat{V}(x_\mathbf{i}, \tau), D_x^-\hat{V}(x_\mathbf{i}, \tau)\big)d\tau;$
> $\qquad \hat{V}(x_\mathbf{i}, t_k) \leftarrow \min\Big\{\hat{V}(x_\mathbf{i}, t_k), l(x_\mathbf{i}, t_k)\Big\};$
> $\qquad \hat{V}(x_\mathbf{i}, t_\mathbf{k}) \leftarrow \max\Big\{\hat{V}(x_\mathbf{i}, t_k), g(x_\mathbf{i}, t_k)\Big\};$

Note that although the two examples we present have two and four vehicles, our method can be done for *any* number of vehicles, as long as the state space of each vehicle is less than six dimensions. The computational complexity of our method scales linearly with the number of vehicles, allowing the possibility of performing trajectory planning for a very large number of vehicles.

V. TWO VEHICLES WITH KINEMATICS MODEL

Consider two vehicles $i = 1, 2$ using the simple kinematics model with the following dynamics in $t \in [t_i^{\text{EST}}, t_i^{\text{STA}}]$:

$$\dot{\mathbf{x}}_i = v_i \mathbf{u}_i(t), \mathbf{u}_i(t) \in \mathcal{U}_i$$
$$\mathbf{x}_i(t_i^{\text{EST}}) = \mathbf{x}_i^0 \tag{14}$$

where $v_1 = v_2 = 1$ are the maximum speeds of the vehicles and $\mathcal{U}_i$ is the unit disk. Under this model, each vehicle can move in any direction at some maximum speed. With the above dynamics, the Hamiltonian for each vehicle is

$$H_i(t, \nabla_{\mathbf{x}_i} V_i(\mathbf{x}_i, t), V_i(\mathbf{x}_i, t)) = \min_{\mathbf{u}_i}\{v_i \mathbf{u}_i(t) \cdot \nabla V(\mathbf{x}_i, t)\} \tag{15}$$

giving the optimal control

$$\mathbf{u}_i(t) = -\frac{\nabla_{\mathbf{x}_i} V_i(\mathbf{x}_i, t)}{\|\nabla_{\mathbf{x}_i} V_i(\mathbf{x}_i, t)\|_2} \tag{16}$$

The vehicles have the following scheduled times of arrival from the following initial conditions:

$$\mathbf{x}_1^0 = (-0.5, 0), \mathbf{x}_2^0 = (0.5, 0)$$
$$t_1^{\text{STA}} = t_2^{\text{STA}} = 0 \tag{17}$$

The target sets of the vehicles are squares with side length 0.2 on the opposite side of the domain, and the obstacles are rectangles near the middle of the domain. The system's initial conditions and domain are shown in Figure 2.

For this system, we determine $t_1^{\text{LST}}, t_2^{\text{LST}}$, the latest acceptable times that vehicles $1, 2$ must depart from their initial
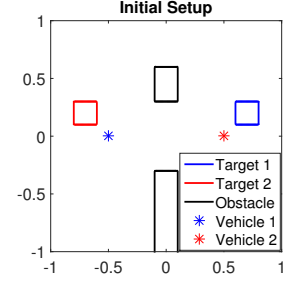

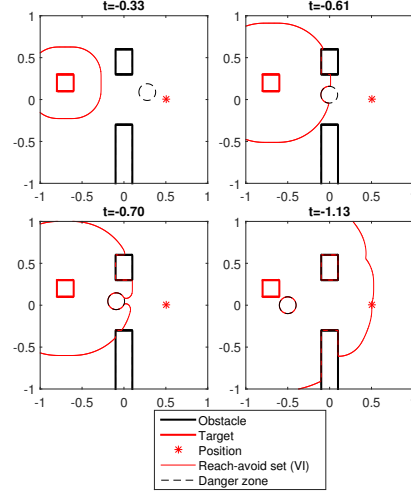Fig. 2: Initial configuration of the two-vehicle example.

Fig. 3: Evolution of reach-avoid set for vehicle 2. The initial reach-avoid set at time 0 grows backwards in time unobstructed before it encounters obstales (left top). When the time reaches $t = -0.61$, the growth of the reach-avoid set is inhibited by both the static obstacle Ω_{obs} and the time-varying obstacle induced by vehicle 1, $\mathcal{O}_1^1$. The evolution of the reach-avoid set is computed until $t = t_2^{\text{LST}} = -1.13$, when the reach-avoid set contains vehicle 2's initial position.

positions $\mathbf{x}_1^0, \mathbf{x}_2^0$ in order to reach their respective targets $\mathcal{T}_1, \mathcal{T}_2$ while avoiding danger. We will do this by computing the reach-avoid sets from the target sets using two different methods. First, we perform SPP by solving the HJI VI (8) for the two vehicles as outlined in Section III. Second, note that this system has a 4D joint state space, and thus the single-obstacle HJI VI (2) would actually be numerically tractable. Therefore, we will also use compute the reach-avoid set by solving (2) in 4D for comparison.

A. Solution via double-obstacle HJI VI and SPP

With the HJI VI and SPP approach, we first determine the minimum time trajectory for vehicle 1 from $\mathbf{x}_1^0$ to $\mathcal{T}_1$. Then, given this trajectory, we determine the optimal trajectory for vehicle 2 that brings vehicle 2 from $\mathbf{x}_2^0$ to $\mathcal{T}_2$ while avoiding the danger zone of vehicle 1.

Figure 3 shows the reach-avoid set for vehicle 2 at various times. We start at $t = t_2^{\text{STA}} = 0$, and propagate the reach-avoid set backwards in time until $t = t_2^{\text{LST}} = -1.13$. Before the induced obstacle touches the reach-avoid set, the reach-
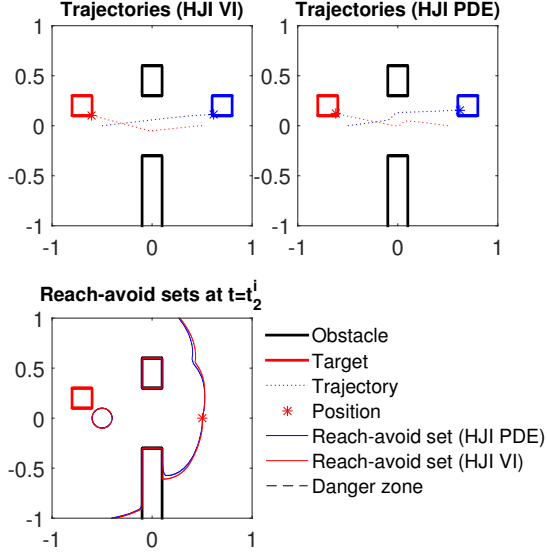
Fig. 4: A comparison between the single-obstacle and double-obstacle HJI VI solutions. With the double-obstacle HJI VI solution, vehicle 2 optimally moves to $\mathcal{T}_2$ while avoiding vehicle 1, which takes the shortest path to $\mathcal{T}_1$. With the single-obstacle HJI VI solution, both vehicles avoid each other along the way to the targets. The resulting reach-avoid sets at $t = t_2^{\text{LST}}$ are very similar in both cases.

avoid set grows from the target set in the same way as in a front propagation problem with uniform speed; this is shown in the left top subplot. Eventually, the obstacle inhibits the propagation of the reach-avoid set, shown in the next two subplots. Finally, the reach-avoid set grows to contain $\mathbf{x}_2^0$, and the computation is stopped at $t_2^{\text{LST}} = -1.13$. The left top plot of Figure 4 shows the resulting trajectory from applying the optimal control in Equation (13).

Computations were done on a 200^2 grid. Trajectory planning for vehicle 1 took approximately 0.34 seconds using the fast marching method [14]. Trajectory planning via solving Equation (8) for vehicle 2 given the trajectory for vehicle 1 took approximately 25 seconds. Computations were done on a Lenovo T420s laptop with a Core i7-2640M processor. This is orders of magnitude faster than doing a 4D HJI calculation, which took approximately 30 minutes.

B. Solution via single-obstacle HJI VI

To solve the single-obstacle HJI VI (2), we define, in the joint state space of the vehicles, the *static* joint target set

$$\mathcal{T} = \{(\mathbf{x}_1, \mathbf{x}_2) \in \mathbb{R}^4 : \mathbf{x}_1 \in \mathcal{T}_1 \wedge \mathbf{x}_2 \in \mathcal{T}_2\} \quad (18)$$

Next we define, also in the joint state space of the vehicles, the *static* joint avoid set

$$\mathcal{A} = \{(\mathbf{x}_1, \mathbf{x}_2) \in \mathbb{R}^4 : \mathbf{x}_1 \in \Omega_{obs} \vee \mathbf{x}_2 \in \Omega_{obs} \\ \vee \|\mathbf{x}_1 - \mathbf{x}_2\|_2 \leq R_C\} \quad (19)$$

Now, we can solve the single-obstacle HJI VI (2) with the terminal set $\mathcal{T} \backslash \mathcal{A}$, and the avoid set $\mathcal{A}$.

The result of solving (2) is shown in the top right and bottom left subplots of Figure 4. The top right subplot shows the resulting trajectory, in which the two vehicles cooperatively avoid collision. The bottom left plot compares the reach-avoid sets computed from solving (2) and the double-obstacle HJI VI (8) at $t = t_2^{\text{LST}}$. The two sets are quite similar. The discrepancy between the reach-avoid sets is due to the difference in control strategies derived from the two different approaches: with the single-obstacle HJI VI, we compute the joint optimal control for both vehicles, and with the double-obstacle HJI VI, we compute the optimal control for vehicle 2 given vehicle 1's optimal trajectory, which does not take into account vehicle 2's motion.

For the latest start time, we get $t_2^{\text{LST}} = -1.15$ from the HJI PDE (recall $t_2^{\text{LST}} = -1.13$ from the HJI VI). This discrepancy is likely due to the grid resolution limitation when doing a 4D calculation. Computations were done on a 45^4 grid, and took approximately 30 minutes.

VI. Four Vehicles with Constrained Turn Rate

Consider four vehicles with states $\mathbf{x}_i = [x_i, y_i, \theta_i]^\top$ modeled using a horizontal kinematics model with the following dynamics for $t \in [t_i^{\text{EST}}, t_i^{\text{STA}}], i = 1, 2, 3, 4$:

$$\begin{aligned}
\dot{x}_i &= v_i \cos(\theta_i) \\
\dot{y}_i &= v_i \sin(\theta_i) \\
\dot{\theta}_i &= \omega_i \\
\mathbf{x}_i(t_i^{\text{EST}}) &= \mathbf{x}_i^0 \\
|\omega_i| &\leq \bar{\omega}_i
\end{aligned} \quad (20)$$

where (x_i, y_i) is the position of vehicle i, θ_i is the heading of vehicle i, and v_i is the speed of vehicle i. The control input $\mathbf{u}_i$ of vehicle i is the turning rate ω_i, whose absolute value is bounded by $\bar{\omega}_i$. For illustration purposes, we chose $\bar{\omega}_i = 1 \ \forall i$. We assume that v_i is constant for this example, but our method can easily handle the case where v_i is a control input. The Hamiltonian associated with vehicle i is

$$\begin{aligned}
&H_i(t, \nabla_{\mathbf{x}_i} V_i(\mathbf{x}_i, t), V_i(\mathbf{x}_i, t)) \\
&= \min_i \big\{ v_i \nabla_x V_i(\mathbf{x}_i, t) \cos(x_i(t)) \\
&\quad + v_i \nabla_y V_i(\mathbf{x}_i, t) \sin(y_i(t)) + \nabla_\theta V_i(\mathbf{x}_i, t) \omega_i \big\}
\end{aligned} \quad (21)$$

giving the optimal control

$$\omega_i(t) = -\bar{\omega}_i \frac{\nabla_{\theta_i} V_i(\mathbf{x}_i, t)}{|\nabla_{\theta_i} V_i(\mathbf{x}_i, t)|} \quad (22)$$

The vehicles have initial conditions and STA as follows:

$$\begin{aligned}
\mathbf{x}_1^0 &= (-0.5, 0, 0), & t_1^{\text{STA}} &= 0 \\
\mathbf{x}_2^0 &= (0.5, 0, \pi), & t_2^{\text{STA}} &= 0.2 \\
\mathbf{x}_3^0 &= \left(-0.6, 0.6, \frac{7\pi}{4}\right), & t_3^{\text{STA}} &= 0.4 \\
\mathbf{x}_4^0 &= \left(0.6, 0.6, \frac{5\pi}{4}\right), & t_4^{\text{STA}} &= 0.6
\end{aligned} \quad (23)$$

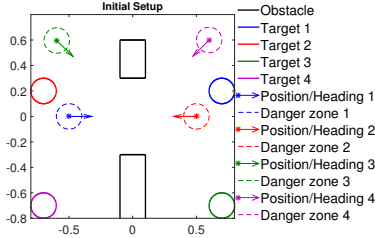Figure 5 shows the initial configuration of this example.

Fig. 5: Initial configuration of the four-vehicle example.

The target sets $\mathcal{T}_i$ of the vehicles are all 4 circles of radius 0.1 in the domain. The centers of the target sets are at $(0.7, 0.2), (-0.7, 0.2), (0.7, -0.7), (-0.7, -0.7)$ for vehicles $i = 1, 2, 3, 4$, respectively. The domain Ω and obstacles Ω_{obs} are the same as those of the example in Section V. The setup for this example is shown in Figure 8.

The joint state space of this system is twelve-dimensional, intractable for analysis using the single-obstacle HJI VI (2). Therefore, we will repeatedly solve the double-obstacle HJI VI (8) to compute the reach-avoid sets from targets $\mathcal{T}_i$ for vehicles $1, 2, 3, 4$, in that order, with moving obstacles induced by vehicles $j = 1, \ldots, i-1$. We will also obtain $t_i^{\text{LST}}, i = 1, 2, 3, 4$, the latest acceptable departure times for each vehicle in order to reach $\mathcal{T}_i$ by t_i^{STA}.

Figures 6, 7, and 8 show the results. Since the state space of each vehicle is 3D, the reach-avoid set is also 3D. To visualize the results, we slice the reach-avoid sets at the initial heading angles θ_i^0. Figure 6 shows the reach-avoid set slices for each vehicle at its latest start times $t_1^{\text{LST}} = -1.12, t_2^{\text{LST}} = -0.94, t_3^{\text{LST}} = -1.48, t_4^{\text{LST}} = -1.44$ determined from our method. The obstacles in the domain Ω_{obs} and the obstacles induced by other vehicles inhibit the evolution of the reach-avoid sets, carving out thin "channels" that separate the reach-avoid set into different "islands". One can see how these channels and islands form by looking at the time evolution of the reach-avoid set, shown in Figure 7 for vehicle 3.

Finally, Figure 8 shows the resulting trajectories of the four vehicles. The subplot labeled $t = -0.55$ shows all four vehicles in close proximity without collision: each vehicle is outside of the danger zone of all other vehicles. The actual arrival times of vehicles $i = 1, 2, 3, 4$ are $0, 0.19, 0.34, 0.31$, respectively. It is interesting to note that for some vehicles, the actual arrival times are earlier than the planned arrival times $t_i^{\text{STA}}, i = 1, 2, 3, 4$. This is because in order to arrive at the target by t_i^{STA}, these vehicles must depart early enough to avoid major delays resulting from the induced obstacles of other vehicles; these delays would have lead to a late arrival if vehicle i departed after t_i^{LST}.

VII. Conclusions and Future Work

We have presented a problem formulation that allows us to consider the multi-vehicle trajectory planning problem in a tractable way by planning trajectories for vehicles in order of priority. In order to do this, we modeled higher-priority vehicles as time-varying obstacles. We then solved a double-
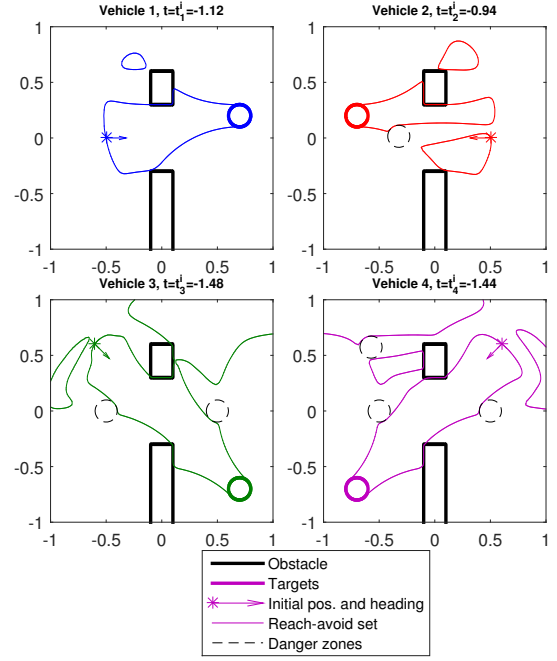

Fig. 6: Reach-avoid sets at $t = t_i^{\text{LST}}$ for vehicles $1, 2, 3, 4$, sliced at initial headings θ_i^0. Since each vehicle has a maximum turn rate constraint, the presence of static obstacles Ω_{obs} and time-varying obstacles induced by higher-priority vehicles $\mathcal{O}_j^i(t)$ carves "channels" in the reach-avoid set, dividing it up into multiple "islands".
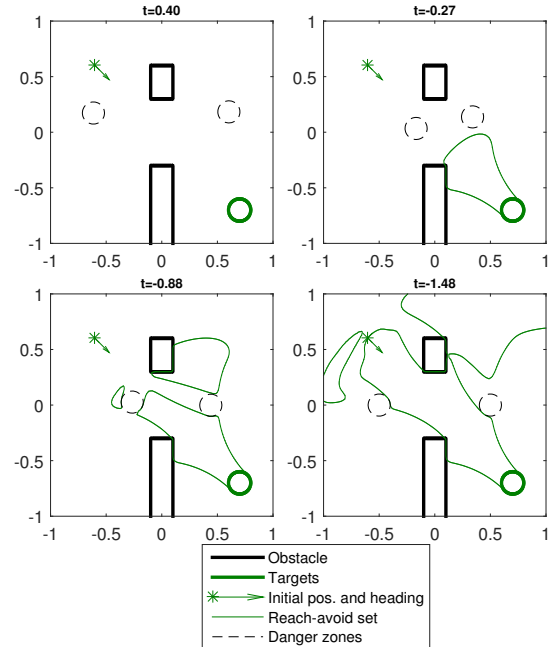

Fig. 7: Time evolution of the reach-avoid set for vehicle 3, sliced at its initial heading $\theta_3^0 = \frac{7\pi}{4}$. Initially, the reach-avoid set grows unobstructed by obstacles, as shown in the top subplots. Then, in the bottom subplots, the static obstacles Ω_{obs} and the induced obstacles of vehicles 1 and 2, $\mathcal{O}_1^3, \mathcal{O}_2^3$, carves out "channels" in the reach-avoid set.
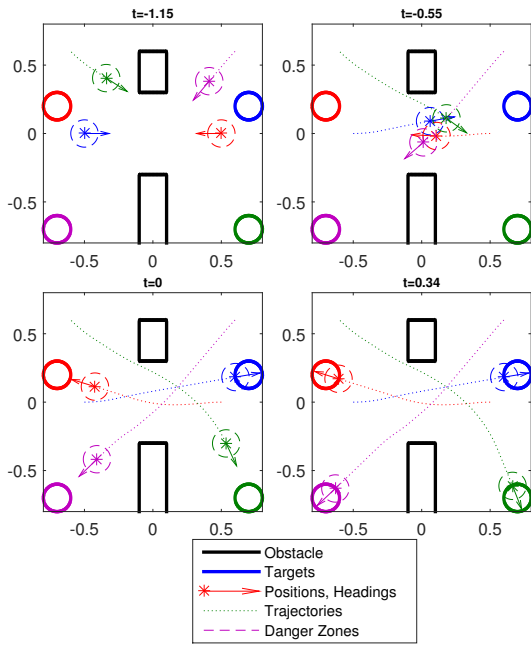
Fig. 8: The planned trajectories of the four vehicles. In the left top subplot, only vehicles 3 (green) and 4 (purple) have started moving; t_i^{LST} is not common across the vehicles. Right top subplot: all vehicles have come within very close proximity, but none is in the danger zone another. Left bottom subplot: vehicle 1 (blue) arrives at $\mathcal{T}_1$ at $t = 0$. Right bottom subplot: all vehicles have reached their destination, some ahead of the scheduled time of arrival t_i^{STA}.

obstacle HJI VI to obtain the reach-avoid set for each vehicle. The solution to the double-obstacle HJI VI characterizes the region from which each vehicle can arrive to its target within a time horizon, while avoiding collision with higher-priority vehicles. The solution also gives each vehicle a latest acceptable departure time as well as the optimal control which guarantees that each vehicle safely reaches its target on time. This paper provides a first application of the double-obstacle HJI VI. Immediate future work includes investigating ways to relax assumptions about the knowledge of the trajectories of other vehicles, more sophisticated induced obstacles for modeling trajectory uncertainty, and problems involving adversarial agents, among other possibilities.

REFERENCES

[1] B. P. Tice, "Unmanned aerial vehicles – the force multiplier of the 1990s," *Airpower Journal*, Spring 1991.
[2] Amazon.com, Inc. (2014) Amazon prime air. [Online]. Available: http://www.amazon.com/b?node=8037720011
[3] J. Stewart. (2014) Google tests drone deliveries in Project Wing trials. [Online]. Available: http://www.bbc.com/news/technology-28964260
[4] Jointed Planning and Development Office (JPDO), "Unmanned aircraft systems (UAS) comprehensive plan – a report on the nation's UAS path forward," Federal Aviation Administration, Tech. Rep., September 2013.
[5] W. M. Debusk, "Unmanned aerial vehicle systems for disaster relief: Tornado alley," in *Infotech@Aerospace Conferences*, 2010.
[6] G. C. Chasparis and J. Shamma, "Linear-programming-based multi-vehicle path planning with adversaries," in *Proceedings of American Control Conference*, June 2005.
[7] P. Fiorini and Z. Shillert, "Motion planning in dynamic environments using velocity obstacles," *International Journal of Robotics Research*, vol. 17, pp. 760–772, 1998.
[8] J. van den Berg, M. Lin, and D. Manocha, "Reciprocal velocity obstacles for real-time multi-agent navigation," in *Robotics and Automation, 2008. ICRA 2008. IEEE International Conference on*, May 2008, pp. 1928–1935.
[9] R. Olfati-Saber and R. M. Murray, "Distributed cooperative control of multiple vehicle formations using structural potential functions," in *in IFAC World Congress*, 2002.
[10] Y.-L. Chuang, Y. Huang, M. D'Orsogna, and A. Bertozzi, "Multi-vehicle flocking: Scalability of cooperative control algorithms using pairwise potentials," in *Robotics and Automation, 2007 IEEE International Conference on*, April 2007, pp. 2292–2299.
[11] I. Mitchell, A. Bayen, and C. Tomlin, "A time-dependent Hamilton-Jacobi formulation of reachable sets for continuous dynamic games," *IEEE Transactions on Automatic Control*, vol. 50, no. 7, pp. 947–957, July 2005.
[12] O. Bokanowski, N. Forcadel, and H. Zidani, "Reachability and minimal times for state constrained nonlinear problems without any controllability assumption," *SIAM Journal on Control and . . .*, pp. 1–24, 2010.
[13] E. Barron and H. Ishii, "The Bellman equation for minimizing the maximum cost," *Nonlinear Analysis: Theory, Methods & Applications*, 1989.
[14] J. A. Sethian, "A fast marching level set method for monotonically advancing fronts," *Proceedings of the National Academy of Sciences*, vol. 93, no. 4, pp. 1591–1595, 1996.
[15] S. Osher and R. Fedkiw, *Level Set Methods and Dynamic Implicit Surfaces*. Springer-Verlag, 2002, ISBN: 978-0-387-95482-0.
[16] I. Mitchell, *A Toolbox of Level Set Methods*, 2009, http://people.cs.ubc.ca/ mitchell/ToolboxLS/index.html.
[17] J. Ding, J. Sprinkle, S. S. Sastry, and C. J. Tomlin, "Reachability calculations for automated aerial refueling," in *IEEE Conference on Decision and Control*, Cancun, Mexico, 2008.
[18] H. Huang, J. Ding, W. Zhang, and C. Tomlin, "A differential game approach to planning in adversarial scenarios: A case study on capture-the-flag," in *Robotics and Automation (ICRA), 2011 IEEE International Conference on*, 2011, pp. 1451–1456.
[19] I. Mitchell, "Application of level set methods to control and reachability problems in continuous and hybrid systems," Ph.D. dissertation, Stanford University, 2002.
[20] O. Bokanowski and H. Zidani, "Minimal time problems with moving targets and obstacles," *18th IFAC World Congress*, 2011.
[21] J. F. Fisac, M. Chen, C. J. Tomlin, and S. S. Sastry, *Submitted to 18th International Conference on Hybrid Systems: Computation and Control (under review)*, 2015. [Online]. Available: http://arxiv.org/abs/1410.6445
[22] E. A. Coddington and N. Levinson, *Theory of ordinary differential equations*. Tata McGraw-Hill Education, 1955.
[23] M. L. C. Mike M. Paglione and H. F. Ryan, "Generic metrics for the estimation of the prediction accuracy of aircraft to aircraft conflicts by a strategic conflict probe tool," *Air Traffic Control Quarterly*, 1999.
[24] M. Chen, Z. Zhou, and C. Tomlin, "Multiplayer reach-avoid games via low dimensional solutions and maximum matching," in *Proceedings of the American Control Conference*, 2014.
[25] F. M. Callier and C. A. Desoer, *Linear System Theory*, 1998.
[26] M. G. Crandall, L. C. Evans, and P. L. Lions, "Some properties of viscosity solutions of hamilton-jacobi equations," *Transactions of the American Mathematical Society*, vol. 282, no. 2, p. 487, Apr. 1984.
[27] L. C. Evans and P. E. Souganidis, "Differential games and representation formulas for solutions of Hamilton-Jacobi-Isaacs equations," *Indiana University Mathematics Journal*, vol. 33, no. 5, pp. 773–797, 1984.
[28] E. Barron, "Differential Games with Maximum Cost," *Nonlinear analysis: Theory, methods & applications*, pp. 971–989, 1990.
[29] S. Osher and C.-W. Shu, "High-order essentially nonoscillatory schemes for hamilton-jacobi equations," *SIAM Journal on Numerical Analysis*, vol. 28, no. 4, pp. pp. 907–922, 1991.
[30] S. Osher and R. Fedkiw, *Level Set Methods and Dynamic Implicit Surfaces*. Springer Verlag, 2003.
[31] C.-W. Shu and S. Osher, "Efficient implementation of essentially non-oscillatory shock-capturing schemes," *Journal of Computational Physics*, vol. 77, no. 2, pp. 439 – 471, 1988.